Title: A dichloro-substituted salicylimine as a bright yellow emissive probe for Al^{3+}

Author: Neeraj Ajit Kumar Sharad Kumar Asthana Shweta K.K. Upadhyay

PII: S1010-6030(16)30289-1
DOI: http://dx.doi.org/doi:10.1016/j.jphotochem.2016.06.023
Reference: JPC 10270

To appear in: *Journal of Photochemistry and Photobiology A: Chemistry*

Received date: 22-4-2016
Revised date: 4-6-2016
Accepted date: 22-6-2016

Please cite this article as: Neeraj, Ajit Kumar, Sharad Kumar Asthana, Shweta, K.K.Upadhyay, A dichloro-substituted salicylimine as a bright yellow emissive probe for Al3+, Journal of Photochemistry and Photobiology A: Chemistry http://dx.doi.org/10.1016/j.jphotochem.2016.06.023

A dichloro-substituted salicylimine as a bright yellow emissive probe for Al^{3+}

Neeraj,[a] Ajit Kumar,[b] Sharad Kumar Asthana,[a] Shweta,[a] K. K. Upadhyay[a]*

[a]Department of Chemistry (Centre of Advanced Study), Institute of Science, Banaras Hindu University, Varanasi, Uttar Pradesh-221005, India

[b]Department of Applied Sciences & Humanities, National Institute of Foundry & Forge Technology, Ranchi-834003, Jharkhand, India.

***E-mail:** drkaushalbhu@yahoo.co.in; kku@bhu.ac.in; **Tel:** +91 542-6702488

Graphical Abstract

A dichloro-substituted salicylimine **(SB1)** detected Al^{3+} down to nanomolar level through bright yellow emission.

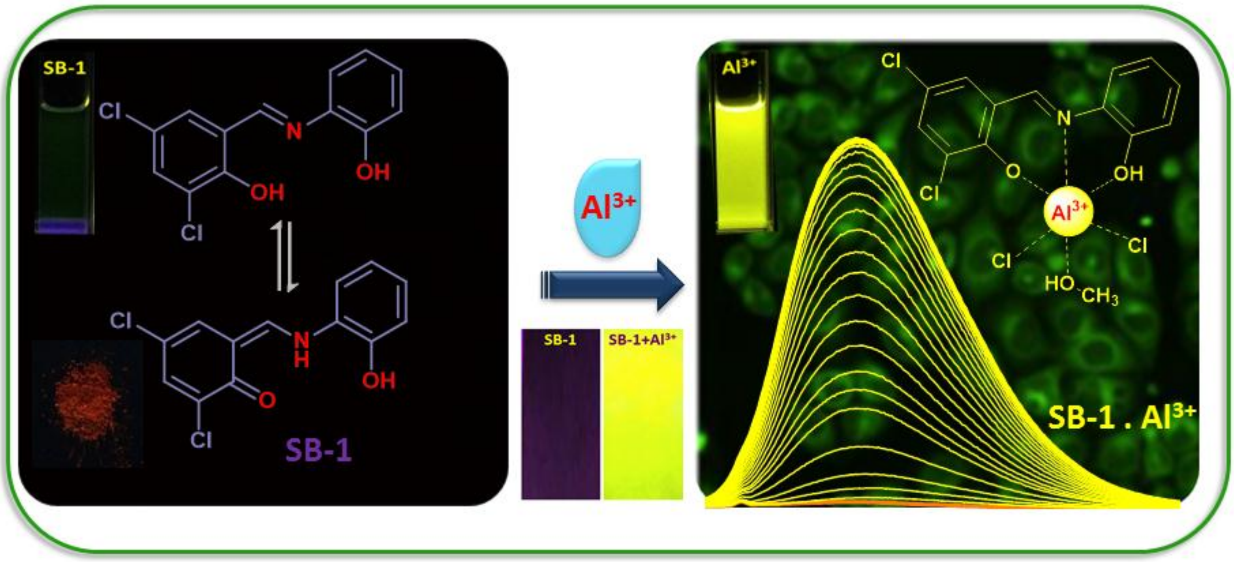

Highlights

- A new fluorescent probe **SB-1** was explored for Al^{3+} with nanomolar detection ability.
- X-ray crystal structure of **SB-1** was also studied.
- This sensing ability was explained by theoretical calculations.
- The **SB-1** was able to illuminate Al^{3+} inside the cells.

Abstract:

A salicylimine based Al^{3+} specific fluorescent turn on probe (**SB-1**) was designed, characterized and evaluated through various spectroscopic techniques. The 1:1 chemical interaction between **SB-1** and Al^{3+} takes place through O-N-O donor sites leading to chelation enhanced fluorescence (CHEF). The lowest detection limit for this measurement was found to be 7.69×10^{-9} M. The binding interaction of **SB-1** with Al^{3+} was studied through ^{1}H & ^{13}C NMR studies, IR as well as through DFT calculations. The HeLa live cells were found to be permeable enough for **SB-1** and was able to detect Al^{3+} inside the cells through confocal microscope.

Keywords: *Fluorescent sensor,* Al^{3+}*, CHEF, Cell Imaging, Density functional Theory*

1. Introduction

Aluminum is well known for its widespread use in daily life because it is the third most prevalent element in the earth crust **[1]**. It plays an important role in many fields, including food packaging, drinking water supplies, cookware, manufacturing industry, and so on **[2]**. According to the World Health Organization (WHO) report, the average daily intake of aluminum in human is around 3–10 mg day^{-1} **[3]**. In spite of its multiple roles in day to day life the aluminum has also been found to be toxic for flora and fauna. A number of diseases associated with the central nervous system like Alzheimer and Dementia etc. are supposed to involve some definite role of Al^{3+} **[4]**. The iron binding protein is known to be the main carrier of Al^{3+} in plasma, and by this way the same crosses the blood-brain barrier and reaches to foetus through placenta **[5]**. Release of free Al^{3+} by the leaching of Aluminum from soil through acid rain is very harmful for growing plants **[6]**. Hence in context of widespread applications and potential toxicity of aluminum, its detection is of great interest.

Most of the available techniques **[7]** for detection of aluminum involve costly instruments, trained technicians and sample preparation. On the other hand the use of optical sensors particularly the fluorescent ones for the detection of trace analytes have come up as strong alternatives of these instrumental methods. A variety of fluorescent sensors for Al^{3+} have been designed by various workers in recent past **[5, 8-10]** mainly upon salicylimine **[5, 8e-h]**, hydrazones **[9]** and acid hydrazine **[10]** frameworks. These designs are in consonance with HSAB principle. The Al^{3+} being a hard acid prefers hard donors like N and O, available through above mentioned compounds. Nevertheless, many of these reported chemosensors have some limitations. On one hand, mostly multiple step synthesis with costly chemicals raise the cost of sensors **[11]**, on the other hand the poor water solubility of the resulting sensors compel the user for inappropriate organic solvents **[12]**. This further reduces the biocompatibility of the sensor making them non suitable for bioassay of Al^{3+} in living cells.

The salicylimine-based optical probes have been an active area of current research as the same offers advantages such as low cost, easier synthetic protocols and better optical responses **[8]**. Recently, our group reported a few fluorescent chemosensors for Al^{3+} based on salicylimine **[13]**. The chemosensors developed for this purpose mostly involves 'O–N–O' coordination site to detect Al^{3+} selectively and with high sensitivity **[8, 13-14]**. Although significant progress has been made in detection of Al^{3+}, still there is a demand for a fluororeceptor of new architecture with improved fluorescent properties. A number of characteristic properties of fluorescent chemosensors *viz.* sensitivity, selectivity, water compatibility, binding constant, biological and environmental applications, sensing mechanisms, are known to be readily influenced by substituents on the benzene ring of salicylaldehyde as well as on amine part.

Although 3,5-dichloro salicylaldehyde is itself already reported as chemosensor for Mg^{2+} ion **[15]** but its Schiff bases with variety of amines were further utilised by different workers for sensing of different ionic and neutral analytes **[16]**. In the same line present report deals with synthesis, characterization and evaluation of a salicylimine based turn-on chemosensor **SB-1** for the fluorescent detection of Al^{3+} by exploiting CHEF process. The nano molar sensitivity and high selectivity of **SB-1** towards Al^{3+} as well as the good permeability in living cells makes the **SB-1** further lucrative.

2. Experimental

2.1 Apparatus:

The IR Spectra for the receptors were recorded on FTIR Spectrophotometer (Model name: spectrum Two; Manufacturer: Perkin Elmer) while ^1H NMR and ^{13}C NMR spectra for the same were recorded on a FT NMR Spectrometer (Model Name: JEOL AL 300, Manufacturer: JEOL Japan); Mass spectrometric analysis was carried out on a MDS Sciex API 2000 LCMS/Brukar Compass data analysis spectrometer. UV-vis. absorption spectra were recorded at 25°C using UV-Visible spectrophotometer (Model Name: UV-1800, Manufacturer: SHIMADZU CORPORATION, ANALYTICAL & MEASURING INSTRUMENTS DIVISION) while the emission spectra were recorded on Fluorolog R -3 spectrofluorometer (Model Name: FL3-11, Manufacturer: JY HORIBA Scientific). Mass spectrometric analysis was carried out on Bruker amaZon SL spectrometer using ultrascan mode (Bruker Daltonics, Bremen, Germany).

2.2. General Methods:

All titration experiments were carried at room temperature. All the metal ions (Al^{3+}, Na^{+}, K^{+}, Ca^{2+}, Mg^{2+}, Ba^{2+}, Cr^{3+}, Mn^{2+}, Fe^{3+}, Co^{2+}, Ni^{2+}, Cu^{2+}, Zn^{2+}, Cd^{2+}, Hg^{2+} and Pb^{2+}) were used as their chloride salts. The ^{1}H NMR spectra were recorded by using tetramethylsilane (TMS) as an internal reference standard. For ^{1}H NMR titration spectra, 5×10^{-3} M solution of **SB-1** was prepared in DMSO-d_6 while the stock solution of Al^{3+} was prepared in D_2O.

For UV-visible/fluorescence titration experiments, the solutions of metal ions were prepared in methanol, except Al^{3+} which was prepared in aqueous medium. Chloride salt of metal ions was used for solution preparation. Due to insufficient solubility of receptors in pure ethanol, its stock solution of 1.0 mM was prepared in DMSO which was used at 10µM and 1µM concentration in ethanol for UV-Visible and fluorescence titration experiment respectively through dilution.

2.3. X-ray diffraction studies

Single crystals of the receptor **SB-1** was grown by slow evaporation of saturated solution of receptor **SB-1** in DMF over a period of few weeks. The single crystal X-ray diffraction measurements were carried out on an Oxford Diffraction Xcalibur system with a Ruby CCD detector as well as on a Bruker SMART APEX CCD diffractometer using graphite-monochromated MoKa radiation (k = 0.71073 Å). All the determinations of unit cell and intensity data were performed with graphite-monochromated Mo-Kα radiation (λ=0.71073 A°). The structures were solved by direct methods, using Fourier techniques and refined by full-matrix least-squares on F^2 using the SHELXTL-97 program package **[17]**. Crystal data and details of the structure determination for receptor **SB-1** are summarized in **ESI, Table S1**.

*2.4. Synthesis of (E)-2,4-dichloro-6-(((2-hydroxyphenyl)imino)methyl)phenol (**SB-1**):*

The **SB-1** was synthesized by a simple Schiff base condensation was characterized by various spectrometric techniques; like FT-IR, ^{1}H & ^{13}C NMR along with ESI-MS studies (**ESI; Fig. S1-S4)**. 2.0 mM methanolic solution of 3,5-dichloro-2-hydroxybenzaldehyde was added to a 2.0 mM methanolic solution of 2-aminophenol followed by constant stirring for ~ 2 hours at the room temperature. A red crystalline solid was precipitated which was filtered and washed several times with methanol and finally dried under vacuum over anhydrous $CaCl_2$.

Yield : 80 %; **IR/cm^{-1}**: 3047, 1628, 1499, 1467, 1370, 1301, 1206, 1134, 1041, 747, 567, 489, 450; **^{1}H NMR : (300 MHz, DMSO-*d_6*, TMS): δ** = 15.52 (s, 1H, -OH^2), 10.21 (s, 1H -OH^1), 9.06 (s, 1H, -CH=N), 7.65 (s, 1H, Ar-H), 7.61 (s, 1H, Ar-H), 7.50-7.47 (d, 1H, Ar-H), 7.20-7.15 (m, 1H, Ar-H), 6.94-6.89 (m, 2H, Ar-H); **^{13}C NMR (75 MHz, DMSO-*d_6*, TMS): δ** = 159.54, 158.99, 150.90, 132.36, 131.08, 130.33, 129.13, 122.98, 119.87, 119.74, 119.40, 118.99, 116.65; **ESI-MS:** m/z (100 %) Calc. for $C_{13}H_9Cl_2NO_2$ [M] = 281.0, found ($M-H^+$) =279.9.

*2.5. Synthesis of Al^{3+} complex of **SB-1***

A 2 mL aqueous solution of $AlCl_3$ (0.067g, 0.5 m mol) was added slowly to a magnetically stirred 10 mL methanolic solution of the **SB-1** (0.141 g, 0.5 mmol). The reaction mixture was stirred at room temperature for overnightfollowed by its evaporation under vacuum yielding yellowish ppt. which was finally dried over anhydrous $CaCl_2$. **Yield**: 85%; **IR/cm^{-1}** : 3195, 1625, 1480, 1456, 1385, 1289, 1267, 1233, 1180, 881, 835; **^{1}H NMR** (300 MHz, DMSO-*d*$_6$, TMS): δ ppm = 9.38 (s, 1H, –OH^1), 8.86 (s, 1H, –CH=N), 7.60-6.58 (7H, Ar–H); **^{13}C NMR (75 MHz, DMSO-*d*$_6$, TMS): δ ppm** = 190.50, 158.32, 154.42, 149.40, 147.94, 132.92, 132.65, 131.80, 130.91, 125.52, 121.84, 118.57, 115.61; **ESI MS:** m/z (100 %), Calc. for [**SB1-**H$^+$+Al^{3+}+2Cl$^-$+CH_3OH]$^+$ = 410.9, found m/z = 410.9.

3. Results and discussion

*3.1. Crystallographic details for **SB1:***

The structure of **SB-1** was confirmed through its single crystal X-ray analysis. Crystals of **SB-1** were obtained by slow evaporation of its saturated DMF solution. The **SB-1** crystallizes into a monoclinic lattice with space group P1. The **SB-1** incorporates two benzene rings and azomethine groups in a coplanar fashion. The molecule adopts an (E)-configuration about the C=N bond (C7–N1) having bond distance 1.296 Å, which is appreciably close to the reported value (1.300 Å). The hydrogen atom particularly N1H is localized at aldimine N atom and thus the **SB-1** takes tautomeric keto form with the strong intra and intermolecular hydrogen bond interaction N–H----O and O–H----O respectively (Fig. 2b) resulting into a nice supramolecular architectures (Fig. 3a & b). The above structure is further supported by the shortening of the bond C13—O2 to 1.275 Å. On the other hand the bond lengths between C-atom and phenolic O-atom i.e., C5–O1 was found to be 1.336 Å. These observations clearly indicated the presence of only one phenolic –OH group in solid state. While in solution state ^{1}H NMR spectrum of **SB-1** in DMSO-d_6 enabled the visibility of both phenolic protons.

3.2. Colorimetric *and fluorescent properties of **SB-1***

The sensing ability of **SB-1** was tested primarily through UV-visible studies in its 30 μM ethanolic solution. As illustrated in Fig. 4, free **SB-1** exhibited strong absorption bands centred at ~ 358 and ~ 467 nm due to $\pi - \pi^*$ and $n - \pi^*$ transitions respectively. The band at ~ 467 nm underwent blue shifting by ~ 42 nm upon concomitant additions of Al^{3+} ion (0–15 equiv.). At this stage slight change in the colour of the solution was observed from light yellow to olive green (Inset, Fig. 4). The isosbestic points at ~ 445 nm further confirmed the formation of the **SB-1**.Al^{3+} complex. The separate additions of 10 equiv. each of a number of metal ions viz., Na^+, K^+, Ca^{2+}, Mg^{2+}, Ba^{2+}, Cr^{3+}, Mn^{2+}, Fe^{3+}, Co^{2+}, Ni^{2+}, Cu^{2+}, Zn^{2+}, Cd^{2+}, Hg^{2+} and Pb^{2+} as their chloride salts to **SB-1** did not show selective colour change for any particular metal ion. Thus **SB-1** was not specific for any particular ion either by naked-eye or by UV-visible spectral changes **(ESI; Fig. S5a & b)**.

The above observations prompted us to check emission spectral pattern of **SB-1** against above mentioned cations. Single crystal X-ray diffraction revealed that **SB-1** exists in keto-enamine form in solid state while ^{1}H NMR spectral studies indicated its enol-imine form in solution state. This enol imine - keto enamine tautomerism through intramolecular proton transfer, PET and allowed C=N isomerization are the major reasons behind weak fluorescent nature of **SB-1 [13, 18]**. However, weakly fluorescent ethanolic solution of SB-1 showed a bright yellow fluorescence emission upon addition of Al^{3+} only, enabling its naked-eye detection under illumination with a UV lamp (Fig 5). The above sensing studies were also performed in EtOH/H_2O mixture up to 2:3; v/v. However, the higher ratio of water affected the fluorescence intensity indicating the dominance of solvent effect over Chelation Enhanced Fluorescence **(ESI; Fig. S6)**.

In order to further understand the chemosensing properties of **SB-1**, the fluorimetric titration was performed with the Al^{3+} ion. The emission spectrum of free **SB-1** showed a very weak single emission band with emission maximum positioned at ~ 530 nm upon its excitation at ~ 420 nm. The fluorescence titration experiments were performed by gradual additions of Al^{3+} into 1.0 μM ethanolic solution of **SB-1**. Upon concomitant additions of Al^{3+} (0-200 equiv.) to the above **SB-1** solution fully developed emission band at ~ 530 nm with nearly 53 fold fluorescence enhancement was observed (Fig. 6).

3.3. Selectivity study

Upon separate respective additions of 40 equivalents of above mentioned metal ions to the ethanolic solution of **SB-1** (1.0 μM), bright yellow fluorescence emission was observed in case of Al^{3+} only (Fig. 7). The fluorescence response of **SB-1**.Al^{3+} ensemble was also studied in the presence of the same metal ions. Upon their respective separate additions only Cu^{2+} and Fe^{3+} showed complete quenching of bright yellow fluorescence of **SB-1**.Al^{3+} ensemble, while metal ions like Ni^{2+}, Co^{2+} showed partial quenching only due to their paramagnetic behaviour **(ESI; Fig. S7a & b)**. Nevertheless negligible effects were noticed upon change of counter anions of Al^{3+} **(ESI; Fig. S8)**.

For the selective fluorescent enhancement of **SB-1** in the presence of Al^{3+} several factors can be listed to rationalize. (i) The chelation of **SB-1** by Al^{3+} leads signal transduction through CHEF. (ii) The binding of Al^{3+} with donor atoms of **SB-1**, ultimately lead to effective locking of PET and cis-trans isomerization around C=N bond. (iii) The hydroxyl group seems to play an important role in the recognition of the Al^{3+} by strengthening the CHEF and hence restricting the C=N isomerization and

PET completely leading to fluorescence enhancement in the form of single emission band at 530 nm. The detection limit of **SB-1** towards Al^{3+} was calculated using fluorescence titration data according to the IUPAC definition **[19]** and the same was found to be 7.68×10^{-9} M with a linearity range of 3.00×10^{-6} to 1.00×10^{-5} M for Al^{3+} **(ESI; Fig. S9)**. This nano molar sensitivity of **SB-1** towards Al^{3+} as well as the high selectivity makes the **SB-1** further lucrative.

3.4. Job's plot analyses and binding stoichiometry

The 1:1 binding stoichiometry of **SB-1** with the Al^{3+} was obtained by the careful analysis of the Job's plot derived from the fluorescence titration experiment (**ESI; Fig. S10**). The corresponding binding constant was determined by the non-linear fitting of fluorescence titration data into 1:1 binding equation **[20]**. The value of the binding constant was found to be $(1.23 \pm 0.19) \times 10^{6}$ with a satisfactory correlation coefficient value, $R^2 = 0.9965$ **(ESI; Fig. S11)**. The same was further confirmed by the ESI-MS of the **SB-1**.Al^{3+} complex which showed a molecular ion peak, at m/z 410.9 for [M] = 410.9, calculated for [**SB1**-H^{+}+Al^{3+}+2Cl^{-}+CH_3OH] **(ESI; Fig. S12)**.

3.5. Binding behaviour of SB-1 towards Al^{3+}

The FTIR measurements indicated binding of imine and hydroxyl groups of **SB-1** with the Al^{3+}. The aldimine absorption was lowered in terms of wavenumber (from 1628 to 1625 cm^{-1}) upon the interaction of Al^{3+} with **SB-1 (ESI; Fig. 13)**. For having further insight into the binding event of **SB-1** with Al^{3+}, ^{1}H NMR titration experiment was performed. Significant spectral changes were observed upon the addition of Al^{3+} (as its chloride salt) to the DMSO-d_6 solution (5×10^{-3} M) of **SB-1**. The peaks for –OH1 at 10.17 δ ppm shifted marginally upfield to 10.04 δ ppm, nevertheless the peak for –OH2 proton at 15.48 δ ppm underwent downfield shift and finally disappeared upon addition of different aliquots of Al^{3+}. The aromatic protons also exhibited marginal upfield shifting (Fig. 8). The same conclusion was further supported by ^1H NMR spectrum of isolated Al^{3+} complex of **SB-1 (ESI; Fig. S14)**. The corresponding ^{13}C NMR spectrum of the **SB-1**.Al^{3+} ensemble showed peak at 190.50 for partial double bond character in C-O bond due to deprotonation of phenolic proton OH2 upon binding with Al^{3+} **(ESI; Fig. S15)**. The same further supported our above speculation regarding the binding of **SB-1** and Al^{3+}.

Thus, on the basis of aforementioned experimental supports from various spectroscopic techniques, the most probable binding mode of Al^{3+} with **SB-1** can be proposed as follows (Fig. 9).

3.6. Density functional theory (DFT) studies

To get further insight into the binding mechanism of the **SB-1** and Al^{3+} and corresponding blue shift in absorption band of **SB-1** in presence of Al^{3+}, we carried out density functional theory (DFT) calculations with 6-31G** basis sets using Gaussian 03 package **[21]**. According to the above discussion, we proposed a complex with 1:1 stoichiometry and hexa coordinated mode of Al^{3+} with the tridentate ligand **SB-1**, two monodentate chloride ions and one monodentate methanol. The optimized configuration of the Al^{3+} complex indicated that the bond length between Al^{3+} and O2 of **SB-1** was 1.825 while Al^{3+} and O1 distance observed was 2.127 Å , very close to Al–N distance (2.065 Å) (Fig. 10).

The optimized structure of **SB-1** shows almost homogeneous electron density pattern in highest occupied molecular orbitals (HOMO) and lowest unoccupied molecular orbitals (LUMO). The **SB-1**.Al^{3+} ensemble exhibited slight heterogeneous electron density pattern in their HOMO. The HOMO-LUMO energy gap also underwent change from 3.0797 to 3.4068 eV. Hence weakening of ICT of **SB-1** in presence of Al^{3+} seems to be responsible for blue shift in the UV-vis. absorption pattern of **SB-1** (Fig. 11).

*3.7. Practical applicability of **SB-1***

3.7.1. Paper test strips

The practical applicability of chemosensor **SB-1** was verified by its incorporation in paper strips. We prepared paper strips by immerging whatman filter paper into the solution of **SB-1** (50 µM) followed by their drying in air. As shown in Fig. 12, **SB-1** strips adopted brownish yellow colour which changed to yellow upon their interaction with Al^{3+}. We also checked fluorescence response of the same under UV light. The **SB-1** strip was non-fluorescent but became bright yellow fluorescent upon its interaction with Al^{3+}. Hence instant qualitative informations regarding Al^{3+} can be obtained through **SB-1** without resorting to instrumental analysis.

3.7.2. Cell imaging Studies

To further validate the feasibility of **SB-1** for the detection of Al^{3+} in vivo, confocal microscope images of HeLa cells incubated with **SB-1** were obtained. As shown in Fig. 13, no fluorescence was observed in HeLa cells upon their incubation with 40 µg mL^{-1} of **SB-1** for 30 minutes. The cells were washed five times with PBS (Phosphate Buffered Saline) buffer solution and 250 µM Al^{3+} was added. The same is well within the range shown to elicit physiological responses (10-500 µM). After further incubation for 5 minutes, an enhancement of the fluorescence in the cells was observed. This is a demonstration of principle test where a significant increase in the intracellular fluorescence intensity was also observed upon increasing the reaction time as the consequence of CHEF as mentioned above also.

4. Conclusion

A salicylimine based ligand **SB-1** was established as a turn “on” fluorescent probe for the selective identification of Al^{3+} in ethanol/ethanol-water mixture. **SB-1** exhibited a fluorescence enhancement upon binding to Al^{3+} due to the combined effect of the CHEF and inhibition of C=N isomerization.The nanomolar detection limit, water compatibility up to 50 % as well as its good permeability in living cells leads to *in vivo* determination of Al^{3+} successfully.

Acknowledgements

KKU acknowledges the financial support from UGC, New Delhi [41-330/2012(SR)]. Neeraj gratefully thanks UPE-JRF for research fellowship (chem./2012-13/154). AK thanks SERB, New Delhi for young Scientist award [YSS/2015/000057]. SKA acknowledges CSIR, New Delhi for JRF/SRF (Aw.No.09/013 (0475)/2012-EMR-I). Shweta acknowledges the financial support from UGC, New Delhi for JRF/SRF (Aw.No.19-12/2010 (i) EU-IV).

References

1. (a) S. Goswami, S. Paul and A. Manna, Selective "naked eye" detection of Al(III) and PPi in aqueous media on a rhodamine–isatin hybrid moiety, RSC Adv. 3 (2013) 10639-10643;

   (b) A. Sahana, A. Benerjee, S. Lohar, A. Banik, S. K. Mukhopadhyay, D. A. Safin, M. G. Babashkina, M. Bolte, Y. Garcia and D. Das, FRET based tri-color emissive rhodamine–pyrene conjugate as an Al^{3+} selective colorimetric and fluorescence sensor for living cell imaging, Dalton Trans. 42 (2013) 13311-13314.

2. (a) M. G. Soni, S. M. White, W. G. Flamm and G. A. Burdock, Safety evaluation of dietary aluminum, Regul. Toxicol. Pharmacol. 33 (2001), 66-79;

   (b) N. W. Bavlor, W. Egan and P. Richman, Aluminum salts in vaccines--US perspective, Vaccine 20 (2002) S18-23.

3. (a) J. Barcelo and C. Poschenrieder, Fast root growth responses, root exudates, and internal detoxification as clues to the mechanisms of aluminum toxicity and resistance: a review, Environ. Exp. Bot. 48 (2002) 75-92;

   (b) B. Valeur and I. Leray, Design principles of fluorescent molecular sensors for cation recognition, Coord. Chem. Rev. 205 (2000), 3-40.

4. (a) B. Wang, W. Xing, Y. Zhao, X. Deng, Effects of chronic aluminum exposure on memory through multiple signal transduction pathways, Environ. Toxicol. Pharmacol. 29 (2010) 308-313;

   (b) D. R. Crapper, S. S. Krishnan and A. J. Dalton, Brain aluminum distribution in Alzheimer's disease and experimental neurofibrillary degeneration, Science 180 (1973) 511-513;

   (c) P. Nayak, Aluminum: Impacts and Disease, Environ. Res. 89 (2002), 101-105.

5. S. Kim, J. Y. Noh, K. Y. Kim, J. H. Kim, H. K. Kang, S.-W. Nam, S. H. Kim, S. Park, C. Kim, and J. Kim, Salicylimine-Based Fluorescent Chemosensor for

Aluminum Ions and Application to Bioimaging, Inorg. Chem. 51 (2012) 3597-3602.

6. (a) R. A. Yokel, The toxicology of aluminum in the brain: a review, Neuro Toxicology 21 (2000) 813-828;

(b) J. Ren, H. Tian, Thermally Stable Merocyanine Form of Photochromic Spiropyran with Aluminum Ion as a Reversible Photo-driven Sensor in Aqueous Solution, Sensors 7 (2007) 3166-3178;

(c) S. H. Kim, H. S. Choi, J. Tian Kim, S. J. Lee, D. T. Quang, J. S. Kim, Novel Optical/Electrochemical Selective 1,2,3-Triazole Ring-Appended Chemosensor for the Al^{3+} Ion, Org. Lett. 12 (2010) 560-563.

7. (a) A. Ceresa, A. Radu, S. Peper, E. Bakker and E. Pretsch, Rational Design of Potentiometric Trace Level Ion Sensors. A Ag^{+}-Selective Electrode with a 100 ppt Detection Limit, Anal. Chem. 74 (2002) 4027-4036;

(b) K. Kimura, S. Yajima, K. Tatsumi, M. Yokoyama and M. Oue, Silver Ion-Selective Electrodes Using π-Coordinate Calix[4]arene Derivatives as Soft Neutral Carriers, Anal. Chem. 72 (2000) 5290-5294;

(c) R. Martinez-Manez and F. Sancenon, Fluorogenic and Chromogenic Chemosensors and Reagents for Anions, Chem. Rev. 103 (2003) 4419-4476.

8. (a) S. Kim, J. Y. Noh, S. J. Park, Y. J. Na, I. H. Hwang, J. Min, C. Kim and J. Kim, Selective fluorescence assay of aluminum and cyanide ions using chemosensor containing naphthol, RSC Adv., 4 (2014) 18094.

(b) S. Mondal, A. K. Bhanja, D. Ojha, T. K. Mondal, D. Chattopadhyay and C. Sinha, Fluorescence sensing and intracellular imaging of Al^{3+} ions by using naphthalene based sulfonamide chemosensor: structure, computation and biological studies, RSC Adv., 5 (2015) 73626.

(c) J. Tian, X. Yan, H. Yang and F. Tian, A novel turn-on Schiff-base fluorescent sensor for aluminum(III) ions in living cells, RSC Adv., 5 (2015) 107012.

(d) S. Das, M. Dutta and D. Das, Fluorescent probes for selective determination of trace level Al^{3+}: recent developments and future prospects, Anal. Methods, 5, (2013) 6262-6285

(e) P. Torawane, K. Tayade, S. Bothra, S. K. Sahoo, N. Singh, A. Borse, A. Kuwar, A highly selective and sensitive fluorescent 'turn-on' chemosensor for Al^{3+} based on C=N isomerisation mechanism with nanomolar detection, Sensor. Actuat. B 222 (2016) 562-566;

(f) J. Y. Noh, S. Kim, I. H. Hwang, G. Y. Lee, J. Kang, S. H. Kim, J. Min, S. Park, C. Kim, J. Kim, Solvent-dependent selective fluorescence assay of aluminum and gallium ions using julolidine-based probe, Dyes Pigm. 99 (2013) 1016-1021;

(g) C. -H. Chen, D.-J. Liao, C.-F. Wan and A.-T. Wu, A turn-on and reversible Schiff base fluorescence sensor for Al^{3+} ion, Analyst 138 *(*2013), 2527-2530;

(h) W.–H. Ding, Wei, Cao, X.-J. Zheng, De-C. Fang, W.-T. Wong and L.-P. Jin, A Highly Selective Fluorescent Chemosensor for Al^{III} Ion and Fluorescent Species Formed in the Solution, Inorg. Chem. 52 (2013) 7320-7322.

9. (a) C. Gou, S.-H. Qin, H.-Q. Wu, Y. Wang, J. Luo, X.-Ya Liu, A highly selective chemosensor for Cu^{2+} and Al^{3+} in two different ways based on Salicylaldehyde Schiff, Inorg. Chem. Comm. 14 (2011) 1622-1625;

(b) A. Ghosh, A. Sengupta, A. Chattopadhyay and D. Das, A single probe for sensing both acetate and aluminum(III): visible region detection, red fluorescence and human breast cancer cell imaging, RSC Adv. 5 (2015) 24194-24199.

10. (a) J.-C. Qin, X.-y. Cheng, K.-C. Yu, R. Fang, M.-f. Wanga and Z.-y. Yang, Design of a novel Schiff-base fluorescent sensor for Al^{3+}: experimental and computational studies, Anal. Methods 7 (2015) 6799-6803;

(b) J. Wanga and Y. Pang, A simple sensitive ESIPT on-off fluorescent sensor for selective detection of Al^{3+} in water, RSC Adv. 4 (2014) 5845-5848;

(c) K. Zhang, Z.-y. Yang, B.-d. Wang, S.-B. Sun, Y.-D. Li, T. Li, Z.-c. Liu, J.-m. An, A highly selective chemosensor for Al^{3+} based on 2-oxo-quinoline-3-carbaldehyde Schiff-base, Spectrochimica Acta Part A: Molecular and Biomolecular Spectroscopy 124 *(*2014) 59-63;

(d) G. J. Park, Y. J. Na, H. Y. Jo, S. A. Lee, A. R. Kim, I. Noh and C. Kim, A single chemosensor for multiple analytes: fluorogenic detection of Zn^{2+} and OAc^{-} ions in aqueous solution, and an application to bioimaging, New J. Chem. 38 (2014) 2587-2594;

(e) L. Fan, T.-r. Li, B.-d. Wang, Z.-y. Yang, C.-j. Liu, A colorimetric and turn-on fluorescent chemosensor for Al(III) based on a chromone Schiff-base, Spectrochimica Acta Part A: Molecular and Biomolecular Spectroscopy 118 (2014) 760-764;

(f) Z.-C. Liao, Z.-Y. Yang, Y. Li, B.-D. Wang, Q.-X. Zhou, A simple structure fluorescent chemosensor for high selectivity and sensitivity of aluminum ions, Dyes Pigm. 97 (2013) 124-128.

11. (a) R. Kang, X. Shao, F. Peng, Y. Zhang, G.-T. Sun, W. Zhao and X.-D. Jiang, A highly selective turn-on fluorescent chemosensor for Al3+ imaging in living cells via through-bond energy transfer, *RSC Adv.* 3 (2013) 21033-21038;

(b) J. Y. Noh, S. I. Kim, H. Hwang, G. Y. Lee, J. Kang, S. H. Kim, J. Min, S. Park, C. Kim and J. Kim, Solvent-dependent selective fluorescence assay of aluminum and gallium ions using julolidine-based probe, Dyes Pigm. 99 (2013) 1016-1021;

(c) Y. K. Jang, U. C. Nam, H. L. Kwon, I. H. Hwang and C. Kim, A selective colorimetric and fluorescent chemosensor based-on naphthol for detection of Al^{3+} and Cu^{2+}, *Dyes P*igm. 99 (2013) 6-13.

12. D. Karak, S. Lohar, A. Sahana, S. Guha, A. Banerjee and D. Das, An Al^{3+} induced green luminescent fluorescent probe for cell imaging and naked eye detection, Anal. Methods 4 (2012) 1906-1908.

13. (a) Neeraj, A. Kumar, V. Kumar, R. Prajapati, S. K. Asthana, K. K. Upadhyay, J. Zhao, A remarkable effect of N,N-diethylamino functionality on the optoelectronic properties of a salicylimine-based probe for Al^{3+}, *Dalton Trans.* 43 (2014) 5831-5839;

(b) V. Kumar, A. Kumar, U. Diwan, Shweta, Ramesh, S. K. Srivastava and K. K. Upadhyay, Salicylideneimines as efficient dual channel emissive probes for Al^{3+}: Harnessing ESIPT and ICT processes, Sensor. Actuat. B 207 (2015) 650-657;

(c) A. Kumar, V. Kumar and K. K. Upadhyay, An Al^{3+} and $H_2PO_4^-$/HSO_4^- selective conformational arrest and bail to a pyrimidine-naphthalene anchored molecular switch, Analyst 13 (2013) 1891-1897;

(d) K. K. Upadhyay and A. Kumar, Pyrimidine based highly sensitive fluorescent receptor for Al^{3+} showing dual signalling mechanism, Org. Biomol. Chem. *8* (2010) 4892-4897.

14. (a) T. Keawwangchai, N. Morakot and B. Wanno, Fluorescent sensors based on BODIPY derivatives for aluminum ion recognition: an experimental and theoretical study, J. Mol. Model. 19 (2013) 1435-1444;

(b) C. H. Chen, D. J. Liao, C. F. Wan and A. T. Wu, A turn-on and reversible Schiff base fluorescence sensor for Al^{3+} ion, Analyst 138 (2013) 2527-2530.

15. G. Men, C. Chen, S. Zhang, C. Liang, Y. Wang, M. Deng, H. Shang, B. Yang and S. Jiang, A real-time fluorescent sensor specific to Mg^{2+}: crystallographic evidence, DFT calculation and its use for quantitative determination of magnesium in drinking water, Dalton Trans. 44 (2015) 2755-2762.

16. (a) G. Men, C. Chen, C. Liang, W. Han and S. Jiang, A novel cascade strategy with supramolecular and chemodosimetric methods for designing a fluorescent ratiometric detector hypersensitive to trace water, Analyst 140 (2015) 5454-5458;

(b) K. Li, A. Tong, A new fluorescent chemosensor for Zn^{2+} with facile synthesis: “Turn-on” response in water at neutral pH and its application for live cell imaging, Sensor. Actuat. B 184 **(**2013) 248-253;

(c) G. Men, G. Zhang, C. Liang, H. Liu, B. Yang, Y. Pan, Z. Wang and S. Jiang, A dual channel optical detector for trace water chemodosimetry and imaging of live cells, Analyst 138 (2013) 2847-2857;

(d) D. Sarkar, S. Jana, P. Karmakar, T. K. Mondal, Quinoline based reversible fluorescent ‘turn-on’ chemosensor for the selective detection of Zn^{2+}: Application in living cell imaging and as INHIBIT logic gate, Sensor. Actuat. *B* 209 2015, 138-146;

(e) P. Mosae Selvakumar, E. Suresh, P. S. Subramanian, Synthesis, spectral characterization and structural investigation on some 4-aminoantipyrine containing Schiff base Cu(II) complexes and their molecular association, Polyhedron 26 (2007) 749-756.

17. (a) G. M. Sheldrick, SHELXL-97, Program for X-ray Crystal Structure Refinement, Göttingen University, Göttingen, Germany, 1997;

(b) G. M. Sheldrick, SHELXS-97, Program for X-ray Crystal Structure Solution, Göttingen University, Göttingen, Germany, 1997.

18. (a) J.-S. Wu, W.-M. Liu, X.-Q. Zhuang, F. Wang, P.-F. Wang, S.-L. Tao, X.-H. Zhang, S.-K. Wu and S.-T. Lee, Fluorescence Turn On of Coumarin Derivatives by Metal Cations: A New Signaling Mechanism Based on C=N Isomerization, Org. Lett. 9 (2007) 33-36;

(b) Z. P. Liu, W. J. He, Z. J. Guo, Metal coordination in photoluminescent sensing, *Chem.* Soc. Rev. 42 (2013) 1568-1600.

19. IUPAC, Spectrochim. Acta Part B 33 (1978) 242- (b) USEPA, Appendix B to Part 136-Definition and Procedure for the Determination of the Method Detection Limit- Revision 1.11, Federal Register 49, 209, 43430, October 26, 1984. Also referred to as "40 CFR Part 136".

20. J. Bourson, J. Pouget and B. Valeur, Ion-responsive fluorescent compounds. 4. Effect of cation binding on the photophysical properties of a coumarin linked to monoaza- and diaza-crown ethers, J. Phys. Chem. 97 (1993) 4552-4557.

21. M. J. Frisch, et al., GAUSSIAN 03, (Revision D.01), Gaussian, Inc., Wallingford, CT (2004).

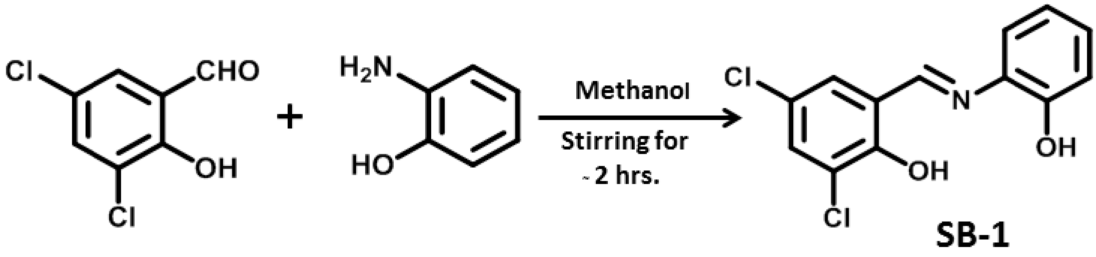

Fig. 1: Synthetic route for receptor **SB-1**

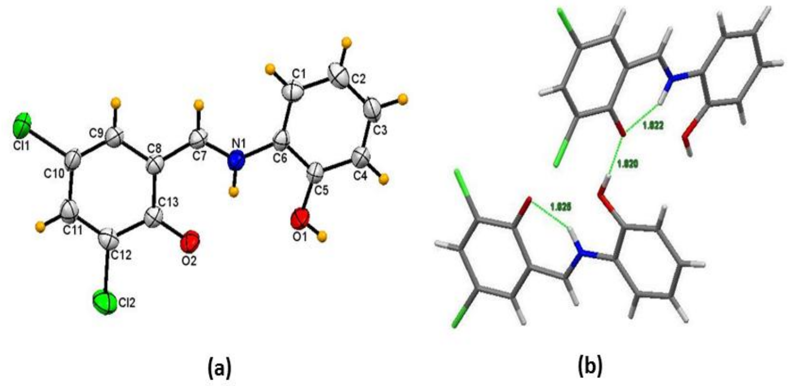

Fig. 2 (a) Single crystal of **SB-1 (b)** Intra and intermolecular hydrogen bonding in **SB-1**.

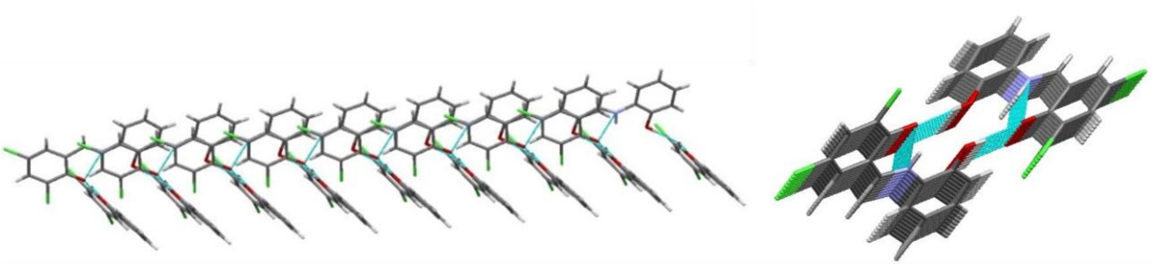

(a) (b)

Fig. 3 (a) & (b) Different modes of supramolecular architecture of **SB-1** through hydrogen bonding.

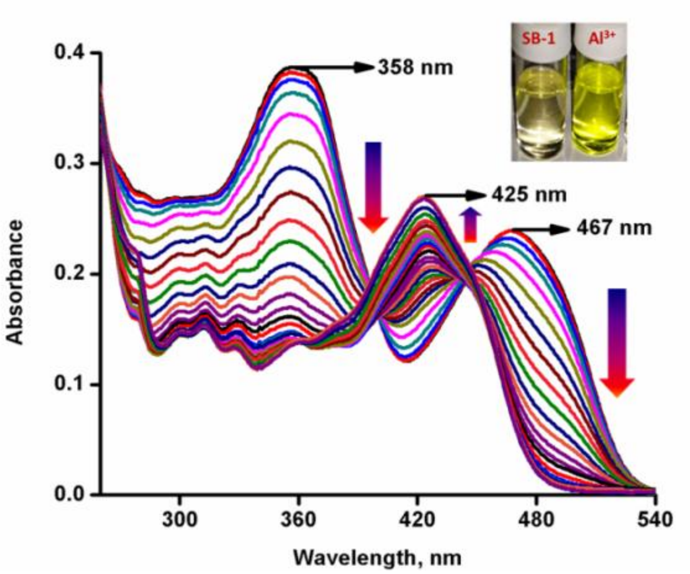

Fig. 4 UV-visible spectral change of 30 μM **SB-1** after addition of Al^{3+} in Ethanol.

[Inset] Visual colour response of **SB-1** and **SB-1**.Al^{3+} ensemble.

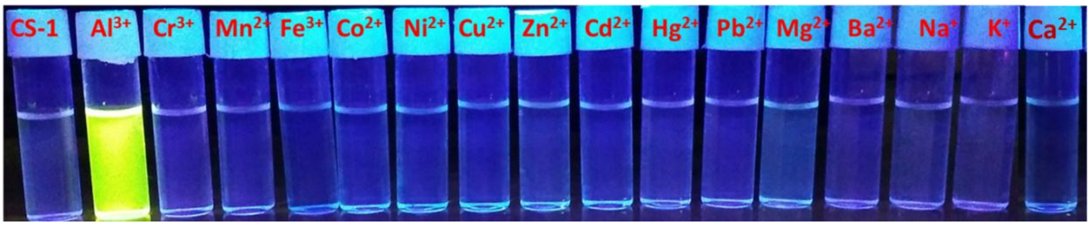

Fig. 5 Visual changes in **SB-1** (10 μM) fluorescence after the addition of 10 equivalents of various metal ions (Under UV-light).

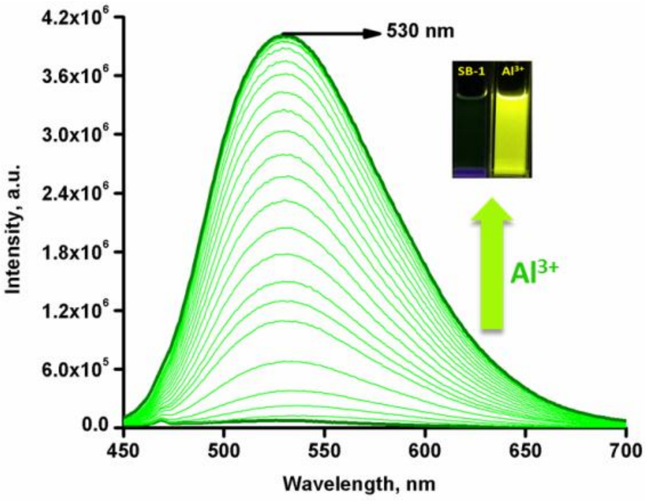

Fig. 6 Fluorescence titration spectra of **SB-1** (1.0 μM) upon incremental addition of Al^{3+} in ethanol. **[Inset]** Visual response of **SB-1** in the presence of Al^{3+} under UV-light.

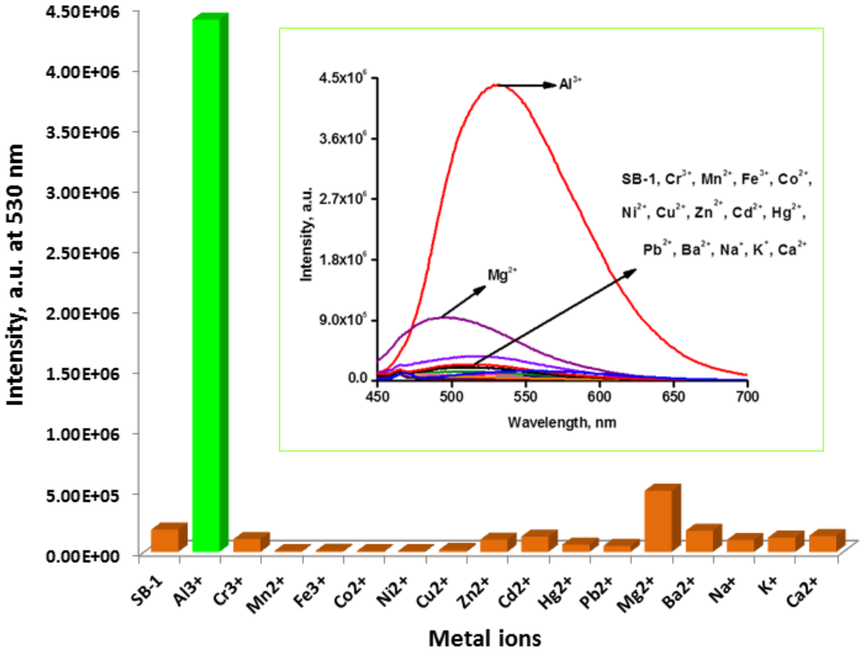

Fig. 7 Graphical representation of fluorescence response of **SB-1** in presence of various metal ions**. [Inset]** Emission spectra of **SB-1** (1.0 µM) in the presence of various metal ions.

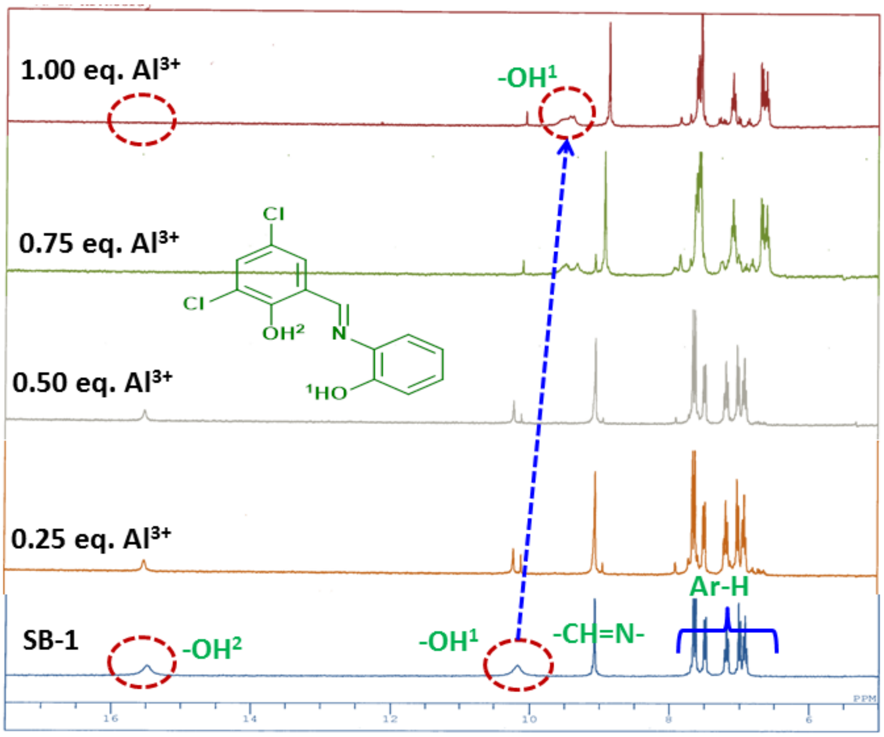

Fig.8 Partial ^{1}H NMR titration experiment of **SB-1** with Al^{3+} ion.

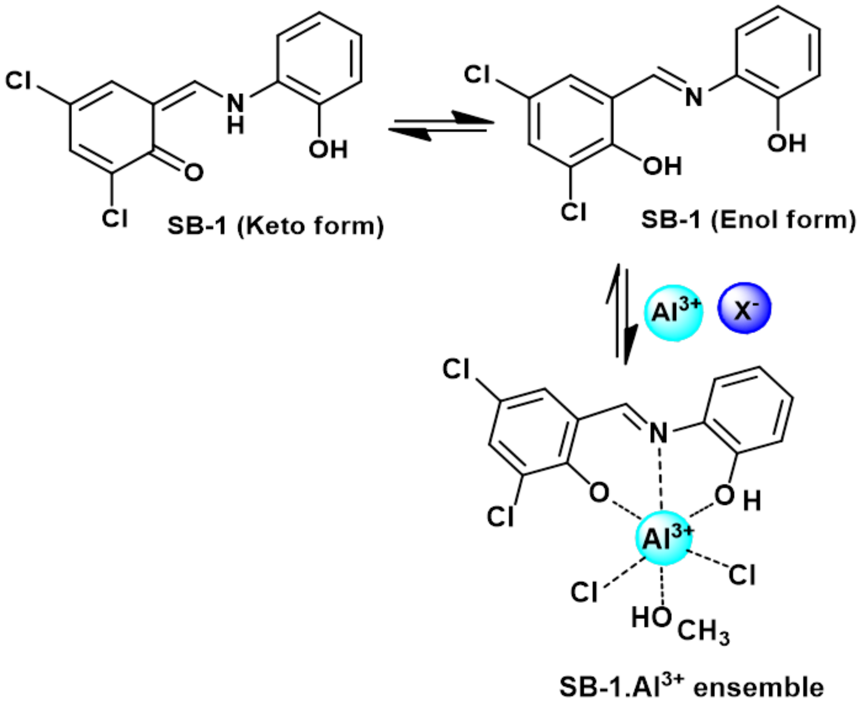

Fig. 9 Proposed mechanism with chemical structure image of **SB-1**.Al^{3+} ensemble.

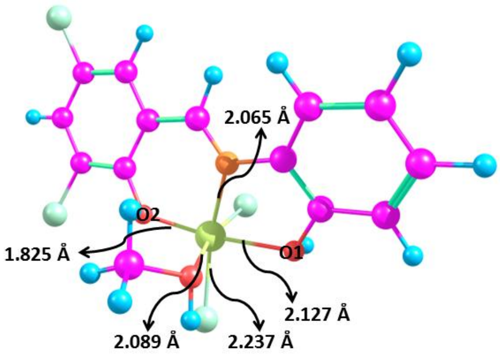

Fig. 10 Optimized structure of Al^{3+} complex of **SB-1**

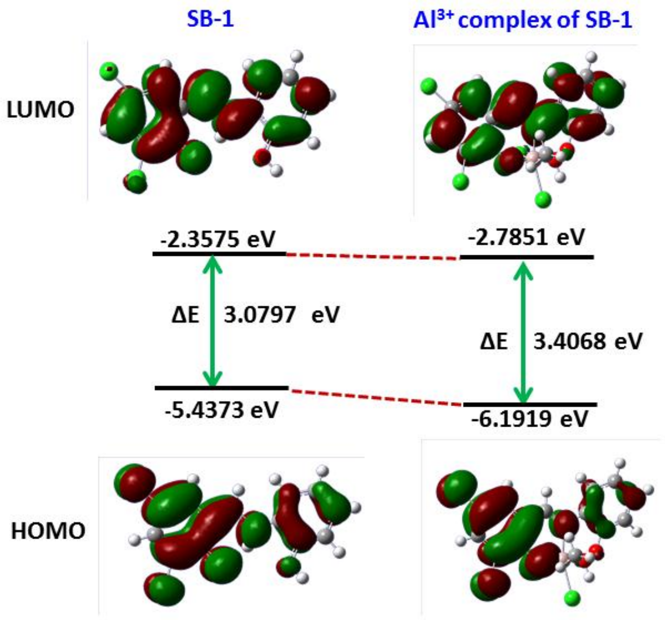

Fig. 11 Energy level diagrams of HOMO and LUMO orbitals of **SB-1** and Al^{3+} complex of **SB-1** calculated on the DFT level using a B3LYP method with 6-31G** basis set.

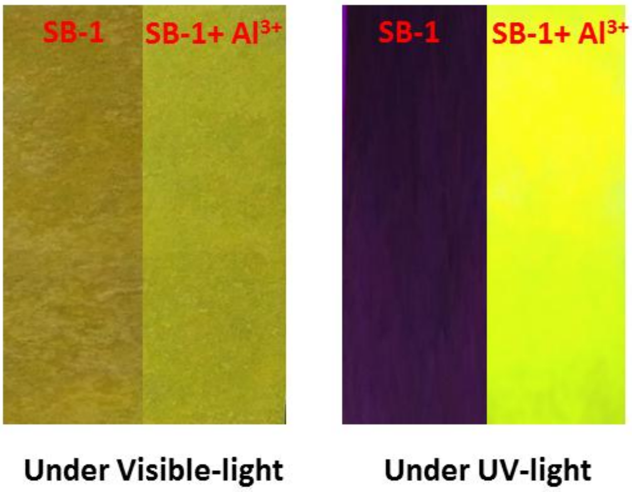

Fig. 12 Demonstration of Al^{3+} sensing by **SB-1** coated paper strips showing response of **SB-1** and **SB-1**.Al^{3+} under visible as well as UV-light.

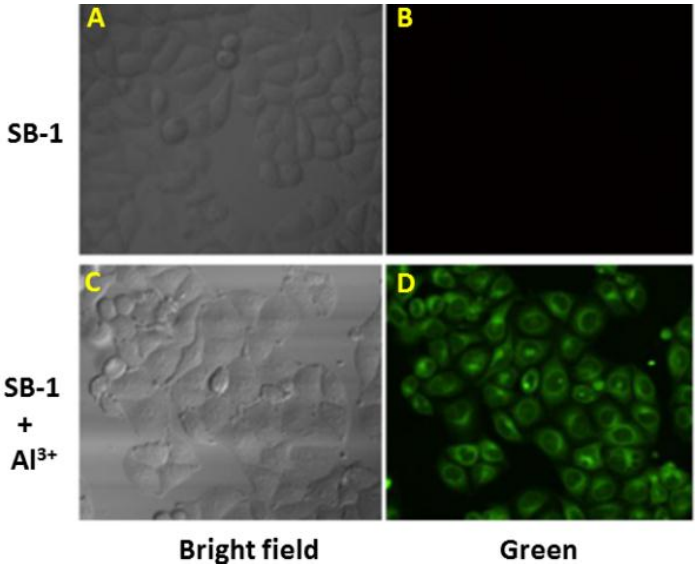

Fig. 13 Representative fluorescence images of HeLa cells, (A and B) cells incubated with 40 µg mL^{-1} **SB-1** for 24 h and (C and D) cells incubated with **SB-1**.Al^{3+} (λ_{ex} = 420 nm).